International Journal of Pharmaceutics 404 (2011) 211–219

Contents lists available at ScienceDirect

International Journal of Pharmaceutics

journal homepage: www.elsevier.com/locate/ijpharm

Pharmaceutical Nanotechnology

Inner ear biocompatibility of lipid nanocapsules after round window membrane application

Ya Zhang[a], Weikai Zhang[a], Marian Löbler[b], Klaus-Peter Schmitz[b], Patrick Saulnier[c], Thomas Perrier[c], Ilmari Pyykkö[a], Jing Zou[a,*]

[a] Department of Otolaryngology, University of Tampere, Medical School, FM1, 3rd Floor, Biokatu 6, 33520 Tampere, Finland
[b] Institute for Biomedical Engineering, University of Rostock, Friedrich-Barnewitz-Str. 4, D-18119 Rostock, Germany
[c] Universiteï d'Angers-INSERM U646 Ingeï nierie de la Vectorisation Particulaire, 49100 Angers, France

ARTICLE INFO

Article history:
Received 27 August 2010
Received in revised form 5 November 2010
Accepted 5 November 2010
Available online 12 November 2010

Keywords:
Cochlea
Molecular pathology
Nanoparticles
Rat
Toxicity

ABSTRACT

Nanoparticle-mediated drug delivery represents the future in terms of treating inner ear diseases. Lipid core nanocapsules (LNCs), 50 nm in size, were shown to pass though the round window membrane (RWM) and reached the spiral ganglion cells and nerve fibers, among other cell types in the inner ear. The present study aimed to evaluate the toxicity of the LNCs in vitro and in vivo, utilizing intact round window membrane delivery in rats. The primary cochlear cells and mouse fibroblast cells treated with LNCs displayed dosage dependant toxicity. In vivo study showed that administration of LNCs did not cause hearing loss, nanoparticle application-related cell death, or morphological changes in the inner ear, at up to 28 days of observation. The cochlear neural elements, such as synaptophysin, ribbon synapses, and S-100, were not affected by the administration of LNCs. However, expression of neurofilament-200 decreased in SGCs and in cochlear nerve in osseous spiral lamina canal after LNC delivery, a phenomenon that requires further investigation. LNCs are potential vectors for the delivery of drugs to the inner ear.

1. Introduction

Hearing loss is a major public health problem and traditional treatment strategies for sensorineural hearing loss (SNHL) are unsatisfactory. Cochlear implant restores the auditory pathway in the context of severe or profound hearing loss. However, hearing performance after implantation is variance (El-Hakim et al., 2002; Gantz et al., 1993; Geers et al., 2002; Osberger et al., 2002). Therefore, an ideal treatment for severe or profound SNHL may depend on novel techniques, such as gene or drug delivery using multifunctional nanoparticles, in addition to cochlear implantation (Pyykko, 2009).

Viral vectors were successful delivered gene to cochlea (Bedrosian et al., 2006; Luebke et al., 2001). Whereas non-viral vector has facilities to targeting by fluorescent tags, surface modification by peptides, and it is economic and easier to produce. Gene expression in inner ear mediated by polyethyleneimine (PEI) was reported (Tan et al., 2008), and sustained drug release in inner ear using poly lactic/glycolic acid (PLGA) nanoparticles was also detected recently (Horie et al., 2010). However, polyethyleneimine were toxic to cells (Florea et al., 2002) and the safety of PLGA nanoparticles need to be investigated. As a controllable drug release system, lipid nanocapsules (LNCs) were shown to distribute in the inner ear after round window membrane application (Zou et al., 2008). Lipid nanocapsules (LNCs) with sizes below 100 nm are biodegradable. They have a lipoprotein-like structure comprising an oily core surrounded by a tensioactive rigid membrane. By varying the core component concentrations, it is possible to control the kinetics of drug release (Jager et al., 2009). LNCs can be stable for six months to one year in suspension (Hureaux et al., 2009; Huynh et al., 2009). These characteristics highlight the potential of lipid nanocapsules for use as nanocarriers.

The biocompatibility of nanoparticles is a major concern in biomedical applications. Toxicological evaluation after systemic administration of LNCs by i.v. injection at a dose of 12 mg/kg/day for 5 consecutive days did not reveal any histological or biochemical abnormalities in mice (Hureaux et al., 2010). After intracochlear application, Scheper et al. (2009) showed that the LNCs were visualized in the rat cochlear cells, although the presence of LNCs did not alter hearing threshold or induce the loss of hair cells. In the present study, we applied LNCs to the round window membrane, which is applauded in the clinic as a minimally invasive approach.

Abbreviations: ABR, auditory brainstem response; DAPI, 4,6-diamidino-2-phenylindole; FITC, isothiocyanate; HE, staining: hematoxylin and eosin staining; IHC, inner hair cells; LNCs, lipid core nanocapsulses; NF-200, Neurofilament-200; OHC, outer hair cells; PBS, phosphate buffered saline; RWM, round window membrane; SGCs, spiral ganglion cells; SGSCs, spiral ganglion Schwann cells; SNHL, sensorineural hearing loss; TRITC, tetramethylrhodamine isothiocyanate.

* Corresponding author. Tel.: +358 331164127; fax: +358 35517710.
E-mail address: Jing.Zou@uta.fi (J. Zou).

0378-5173/$ – see front matter © 2010 Elsevier B.V. All rights reserved.
doi:10.1016/j.ijpharm.2010.11.006

We then evaluated the impact on neural structural elements including neurofilament and S-100, as well as neural functional elements including ribbon synapses and synaptophysin in the cochlea. General cellular viability studies were performed as well.

2. Experimental procedures

2.1. Animals

Two newborn rats were selected for primary cochlear cell culture. Eighteen male Sprague–Dawley rats with normal ABR threshold (auditory brainstem response, supplied by the experimental animal unit, University of Tampere) were used in the study, in accordance with guidelines provided by the local ethics committee of the University of Tampere (permission no: 985/2003). Animal care and experimental procedures were conducted in accordance with European legislation.Ten rats were used for auditory brain stem response measurement, apoptotic analysis and neural structural elements analysis. Three rats were used for neural functional elements analysis. Five rats used as untreated control in analyzing of neural elements.

2.2. Manufacturing LNCs

2.2.1. Initial steps in the manufacture of LNCs

The first step of the formulation involved an emulsion consisting of Labrafac® WL 1349, an oil made of capric and caprylic acid triglycerides (average molecular weight of 512); Lipoïd® S75-3, a soybean lecithin made of 69% phosphatidylcholine and other phospholipids; Solutol® HS 15, another surfactant; polyethylene glycol 660 hydroxystearate (C18E15); and free polyethylene glycol 660. The optimal amounts of ingredients for preparation of 50 nm of LNCs were: Labrafac® (1.028 g), Lipoïd® (0.075 g), Solutol® (0.846 g), NaCl (0.089 g) and pure water (2.962 g). This mixture was prepared under magnetic stirring at room temperature to obtain an emulsion of oil in water. After progressive heating at a rate of 4 °C/min under magnetic stirring, we observed a short interval of transparency at temperatures close to 70 °C, and the inverted phase (water droplets in oil) was obtained at 85 °C. Then, three cycles of cooling and heating were applied between 85 °C and 60 °C at the same rate of 4 °C/min (near the phase inversion zone). Ultimately, rapid dilution in cold water at a temperature close to 0 °C produced a suspension of nanocapsules.

2.2.2. Protocol post-insertion of 15,16 DSPE-PEG2000-amino

LNCs were incubated for 90 min with an aqueous micellar solution of DSPE-PEG-amino at 60 °C. The suspension was vortexed every 15 min and then quenched in an ice bath for 1 min. The final DSPE-PEG concentration corresponded to 6 mol% of total surface molecules (i.e., Solutol and Lipoïd).

2.2.3. FITC and Rhodamine B labeling

After the post-insertion process, 2 mg of FITC (isothiocyanate, 5.13 μmol) was added to 2.95 mL of the LNC suspension, and the pH was increased to 10 by adding a few drops of 0.1 M Na_3PO_4 solution. The sample was protected from light and placed in a water bath under magnetic stirring at 35 °C for 45 min. After the sample was cooled in an ice bath for 3 min in order to stop the reaction, size exclusion chromatography utilizing a Sephadex G-15 column was performed to separate free FITC from labeled LNCs. Optical density (FITC detection) as well as turbidity at 680 nm (LNC detection) were measured for each fraction. Fractions corresponding to the FITC-labeled LNCs were analyzed by dynamic light scattering. Electrokinetic measurements were performed at a constant conductivity (0.03 μs cm^{-1}). These measurements indicated a hydrodynamic diameter of 52 ± 5 nm and a zeta potential of -35 ± 7 mV (for non-labeled LNCs, we obtained diameter of 48.9 nm, zeta potential of 5.0 ± 0.5 mV and concentration of 123 mg/mL). Only fractions with a polydispersity index lower than 0.2 were pooled and used for animal testing. For Rhodamine B labeling, FITC was replaced by 2 mg Rhodamine B.

2.3. In vitro study

2.3.1. L929 mouse fibroblasts

L929 mouse fibroblasts (ATCC number CCL 1, DSMZ, Braunschweig, Germany) were cultured in DMEM culture medium (AppliChem, Darmstadt, Germany) containing 4.5 mg/mL glucose, 10% FCS, 100 U/mL penicillin G, 100 μg/mL streptomycin (PAA Laboratories), and $NaHCO_3$ (3.7 g/L) at 37 °C, 5% CO_2, and 95% humidity. Cells were harvested by trypsinization (PAA Laboratories) and seeded at a density of 2000 cells/well into a 96 well microtiter plate (Greiner Bio-one, Frickenhausen, Germany). After 1 day of cell culture, medium was replaced by 200 μL of freshly prepared nanoparticle suspension in cell culture medium (working solution). After 48 h of cell growth under the above conditions, cell culture medium was replaced by 10% CellQuanti-Blue reagent (BioAssay Systems, Hayward, CA, USA) in cell culture medium. Cells were then incubated for another 2 h. Cellular reductases reduce the CellQuanti-Blue reagent resazurin to resorufin. The extent of reduction was quantified by fluorescence measurements (Fluostar Optima, BMG, Offenburg, Germany; excitation wavelength 544 nm, emission wavelength 590 nm).

Nanoparticle suspensions were diluted into cell culture medium to yield suspensions of 10^{15} nanoparticles/mL (equivalent to 7.85 mg/mL). These suspensions were further diluted with cell culture medium to 7.85 mg/mL, 0.785 mg/mL, 0.785E−1 mg/mL, 0.785E−2 mg/mL, 0.785E−3 mg/mL, 0.785E−4 mg/mL, 0.785E−5 mg/mL, 0.785E−6 mg/mL, 0.785E−7 mg/mL, 0.785E−8 mg/mL (working solution).

Uptake of nanoparticles into cells was followed by fluorescence microscopy (Nikon Eclipse TE300) at an excitation wavelength of 510–560 nm and emission wavelength of >590 nm.

2.3.2. Mixed primary rat cochlear cell culture

Two four-day-postpartum (P4) rats were sacrificed by decapitation after anesthetization with medetomidine hydrochloride (0.8 mg/kg, Domitor, Orion, Finland) and ketamine hydrochloride (80 mg/kg, Ketalar, Pfizer, UK). Four cochleae were dissociated with 1 mg/mL elastase (Sigma–Aldrich, USA), 1 mg/mL collagenase (Worthington, USA), and 0.5 mg/mL trypsin in CMF-PBS for 15 min at 37 °C. Cells were then plated into two 4-well Lab-Tek® II Chamber Slides™ (USA). Cultures were maintained in a defined medium: DMEM-F12 (Gibco, USA) with B27 supplement (Gibco, USA), 1 mM n-acetyl-L-cysteine (Sigma–Aldrich, USA), penicillin–streptomycin (Gibco, USA), and 20 ng/mL epidermal growth factor (Sigma–Aldrich, USA) in a 5% CO_2/5% O_2 humidified incubator.

The cells were incubated for 24 h at 37 °C in medium containing 1.5 mg/mL, 0.15 mg/mL or 0.015 mg/mL LNCs, washed with PBS, incubated with medium containing 5 μg/mL propidium iodide for the analysis of cellular viability, then fixed with 4% PFA followed by DAPI staining (10 ng/mL, Sigma–Aldrich, USA). The slides were mounted with Fluoromount (Sigma–Aldrich, USA) after washes with PBS-T (PBS containing 0.1% Tween-20).

The cells were observed under an Olympus microscope IX70 installed with ANDOR IQ. The excitation filters were 488 nm (blue excitation) and 568 nm (green excitation), with an Ar–Kr laser as the excitation source. The corresponding emission filters were 525/50 (FITC) and 607/45 (propidium iodide). DAPI was excited with a 340–380 nm filter and detected using a 500 LP filter. Dead

cells were identified by positive staining of propidium iodide, which is unable to penetrate the plasmic membrane of viable cells but passes the cellular and nuclear membranes and binds to chrosome DNA in both apoptotic and necrotic cells (Smolewski et al., 2002). The survival rates of LNC-treated cells were normalized to those of untreated cells [survival rate = 1 − (death rate of LNC-treated cells − death rate of untreated cells)]. The fluorescent signal intensities of internalized LNCs in the cytoplasm were measured by Image J software. These signal intensities were normalized to the signal intensity of background. 28 cells for untreated control, 33 cells for the 0.015 mg/mL LNC-treated samples, 30 cells for 0.15 mg/mL LNC-treated samples, 23 cells for 1.5 mg/mL LNC-treated samples, were counted in the study.

2.4. In vivo study

2.4.1. Round window membrane application of LNCs

Animals were fully anesthetized by 0.8 mg/kg medetomidine hydrochloride (Domitor, Orion, Finland) and 80 mg/kg ketamine hydrochloride (Ketalar, Pfizer, UK). The operation was performed under sterile conditions. After local analgesia with lidocaine, a post-auricular incision was used to expose the left bulla. A hole was drilled on the bulla with a 2 mm diameter burr. After visualizing the stapes artery, the round window membrane was identified above the artery. A small piece of gelatin sponge pledget saturated with LNCs or 0.9% NaCl (Baxter, Finland) was placed on the round window membrane (pledget size 8 mm^3 after saturation, LNC concentration: 20.5 g/L, stored at 48 °C for 3 months), and it was left on the RWM of left ear for D28 for ABR study and 2 h for neural elements studies. The hole on the bulla was sealed with muscle and the wound was sutured. Saline (2 mL) was administered through subcutaneous injection to the neck. Antisendan (atipamezole hydrochloride, Orion Pharma, Finland) (2 mg/kg) was injected i.p. after the operation to accelerate recovery from anesthesia. RIMADYL (1.0 mg/kg, Pfizer, UK) and Baytril (10 mg/kg, Orion, Germany) were injected i.p. once a day during the first 3 days after the operation.

2.4.2. Auditory brainstem response measurement

In total, ten rats were used for ABR measurement. The animals were divided according to the treatment: five LNC-treated rats and five negative control rats.

BioSig32 (Tucker Davis Technologies, USA) was used for ABR threshold recording in LNC-treated rats and 0.9% NaCl-treated rats. A click duration of 50 μs and a repetition rate of 21.1/s were used for stimulation with alternative phase. Responses from 500 sweeps were averaged with a gain of 20 at each intensity level, using a filter of 0.1–3 kHz. Thresholds were identified as 3 repeatable responses of wave II (peak II) using visual detection criterion in 5 dB steps. ABR thresholds were measured at six time points. The latency intervals between peak I and peak II ($Interval_{peak\ I–II}$) at 50 dB peak-to-peak equivalent SPL (ppeSPL) were compared among groups or different time points. The time points were as follows: before surgery, 2 h post-administration, 1 week post-administration (D7), 2 weeks post-administration (D14), 3 weeks post-administration (D21), and 4 weeks post-administration (D28).

2.4.3. Morphological study

After the last ABR measurement, animals were perfused with 4% paraformaldehyde (PFA, Sigma–Aldrich, USA) in 0.1 M PBS (pH 7.4) following cardiac perfusion and removal of the blood with 50 mL physiological saline containing 0.3 mL heparin (100 IE). The bullae were collected and fixed with 4% PFA overnight. The cochleae were thoroughly washed with tap water for 30 s and then opened by breaking the bony wall under a stereo microscope. After washing with 0.01 M PBS, the specimens were decalcified with 10% EDTA at room temperature for 4 weeks, embedded with paraffin, and sectioned at 5 μm thickness. After deparaffinization, the slides were stained with hematoxylin–eosin.

2.4.4. Apoptotic analysis

After deparaffinization, the specimens were treated with 0.1% Triton-X100 for 10 min, incubated with 0.1% trypsin for 30 min at 37 °C, irradiated with 0.1 M citrate buffer (PH 6.0) at 350 W microwave irradiation for 5 min, and washed with PBS. As a positive control, tissue was incubated with 0.2 μg/mL proteinase K in 50 mM Tris buffer (pH 7.5) for 10 min at 37 °C. TUNEL mixture [20 μL enzyme solution in 180 μL label solution; In Situ Cell Death Detection Kit (Roche Diagnostic GmbH, Germany)] was applied on slides (50 μL label solution on negative control slides) for 60 min at 37 °C, washed with PBS, and mounted with Aqueous Mounting Medium (Gel Mount™, Sigma–Aldrich, USA).

2.4.5. Neural element analysis-structural elements

After deparaffinization and treatment with 0.1% trypsin as described, the slides were incubated with 1: 20 preimmunized goat serum at room temperature for 60 min and then with either of the following primary antibodies at 4 °C overnight: rabbit anti-neurofilament-200 (NF-200) polyclonal antibody (1: 400 Sigma–Aldrich, USA), rabbit polyclonal antibody to S-100 (1: 400, Abcam, UK), and mouse monoclonal antibody to synaptophysin (1:200, Sigma–Aldrich, USA). After washing with PBS-T, the specimens were incubated with Alexa Fluor-568-labeled goat anti rabbit IgG (1:400, Invitrogen, USA) or tetramethylrhodamine isothiocyanate (TRITC)-labeled goat anti mouse IgG (1:400, Invitrogen, USA) at room temperature for 60 min, followed by incubation with 4,6-diamidino-2-phenylindole (DAPI; 10 μg/mL, Sigma–Aldrich, USA) for 10 min. The slides were mounted with Gel Mount TM Aqueous Mounting Medium (Sigma–Aldrich, USA) after washes with PBS.

2.4.6. Neural element analysis-functional elements

Six cochleae from 3 rats treated with LNCs for 2 h and four cochleae from two untreated rats were employed for ribbon synapse and synaptophysin double staining.

After dissection, the specimens were treated with 0.1 M PBS containing 0.3% Triton-X 100 for 5 min, then immunostaining was conducted as above mentioned, Briefly, specimens were stained with rabbit anti-synaptophysin antibody (1:400, Sigma–Aldrich, USA) at 4 °C overnight, incubated with purified mouse anti-Ctbp2 monoclonal antibody (1:100, BD Transcription Laboratories, USA) overnight at 4 °C, then incubated with corresponding second antibodies [Alexa Fluor-568 labeled goat anti-rabbit IgG (1:400, Invitrogen, USA) or FITC anti-mouse IgG produced in goat (1:400)] for 60 min, and finally stained with DAPI. The lateral wall and modiolus from the basal turn, middle turn and apex were mounted with Aqueous Mounting Medium (Gel Mount™, Sigma–Aldrich, USA) for confocal microscopy.

The whole-mount samples and cross-sections were observed under an Olympus microscope IX70, which had been installed with ANDOR IQ. The excitation filters were 488 nm (blue excitation) and 568 nm (green excitation), with an Ar–Kr laser as the excitation source. The corresponding emission filters were 525/50 (FITC) and 607/45 (TRITC and Alexa 568). DAPI was excited with a 340–380 nm filter and detected using a 500 LP filter. For 3D scanning, the inter-slice thickness was 0.5 μm. The ribbon synapses of the basal turn were counted in three-dimensional images. Seven views in four untreated cochleae and 11 views in 6 LNC-treated cochleae were selected, and only the basal and the lower middle turn were included in the analysis.

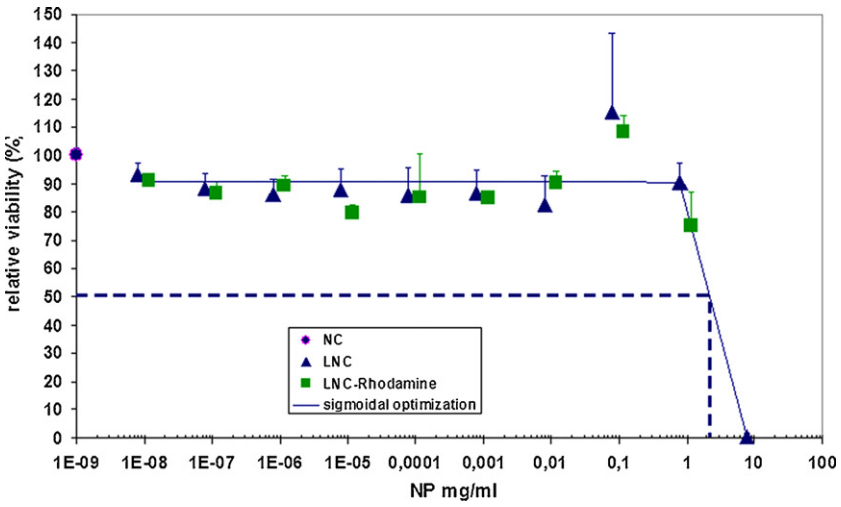

Fig. 1. Cell viability of L929 mouse fibroblasts is dependent on the amount of LNCs applied. The LC_{50} was calculated as 2.2 mg NP/mL (dashed line). NC: untreated control.

2.5. Analysis and statistics

Statistical analyses were performed using the SPSS 11.5 software package. Significant differences were identified using Student's *t*-test. ABR thresholds and $interval_{peak\ I–II}$ were compared between LNCs treated group and NaCl treated group. For NF-200 staining, the signal intensities of cochlear nerve, auditory nerve, and nerve fibers projecting to spiral ganglion cells (SGCs) and inner hair cells (IHCs) were compared between groups. For S-100 staining, the signal intensities of SGC, SL and Deiters' cells were compared between groups. The number of ribbon synapses of basal turn and 2nd turn were compared. A difference was considered to be statistically significant at $p < 0.05$.

3. Results

3.1. In vitro study results

3.1.1. L929 cells

LNCs at concentrations up to 0.785 mg/mL were not toxic to L929 cells (Fig. 1). However, high concentrations of LNCs showed low cytotoxicity, yielding an LC_{50} of 2.2 mg/mL. Identical LNCs labeled with Rhodamine were visualized inside cells. Toxic effects similar to those mediated by unlabeled LNCs (Fig. 1) might be due to the overload phenomenon (Moss, 2006).

3.1.2. Cultivated mixed rat cochlear cells

The survival rates of cells treated with 1.5 mg/mL, 0.15 mg/mL and 0.015 mg/mL LNCs were 37.94%, 86.41%, and 80.06%, respectively. LNC signal intensity in cytoplasm increased with LNC concentration (Fig. 2). For the cells treated with low concentrations of LNCs (0.015 mg/mL), few LNCs were found in the cytoplasm (Fig. 2C). Propidium iodide-positive cells, whether among the 0.15 mg/mL or the 0.015 mg/mL LNC-treated group, exhibited condensed LNCs in the cytoplasm and abnormal morphology. In all three groups of LNC-treated cells, surviving cells had fewer LNCs in cytoplasm.

3.2. In vivo study results

3.2.1. Hearing results

None of the animals experienced middle ear infection during the treatment period.

Immediately after LNC treatment (D0), ABR threshold increases of 11.67 ± 2.89 dB ppeSPL (mean ± SEM) and 8.75 ± 2.50 dB ppeSPL (mean ± SEM) were detected in the NaCl control group and LNC-treated group, respectively. After 7 days of treatment (D7), ABR thresholds were recovered to baseline levels (Fig. 3A). But the ABR threshold variance had no statistical difference ($p > 0.05$, Bonferroni, ANOVA).

The ABR latency interval between peak I and peak II ($Interval_{peak\ I–II}$) at 50 dB ppeSPL was prolonged at D0 in the NaCl group (mean ± SEM, 0.94 ± 0.01 ms) and the LNC-treated group (mean ± SEM, 0.88 ± 0.01 ms) compared to pre-treated levels (mean ± SEM; 0.73 ± 0.03 ms and 0.77 ± 0.01 ms, respectively). However, only the NaCl-treated group was significantly different ($p < 0.01$; Bonferroni, ANOVA). No statistically significant differences were observed in LNC-treated group at D0 ($p > 0.05$, Bonferroni, ANOVA; Fig. 3B).

3.2.2. Morphological results

Light microscopy with HE staining did not reveal any inflammation in the inner ear. The morphology of the inner ear, including the cochlea and vestibule, were preserved after LNC treatment (Fig. 4).

3.2.3. LNC treatment did not induce apoptosis

TUNEL-positive staining was constantly observed in interdental cells and stria marginal cells of the basal and second turns of the cochlea of rats with and without LNC treatment. Positive staining was also occasionally detected in OHCs, IHCs, and semicircular canal (SSC) endothelial cells of rats in both the control and the LNC-treated groups (Fig. 5G–J). TUNEL-positive nuclei appeared throughout the entire cochlea on the positive control slide with much greater intensity than that in the specimens processed with standard protocol (Fig. 5K). No TUNEL-positive staining was detected in the negative control.

3.2.4. The inner ear neural elements were preserved

NF-200 staining in the peripheral processes of SGCs innervating the inner hair cells and the outer hair cells, cochlea nerve in osseous spiral lamina canal, SGCs, and the cochlear nerve in modiolus was well preserved in both the untreated and LNC-treated rats (Fig. 5B and C). The fluorescence signal in SGCs ($p < 0.01$) and in cochlear nerve in osseous spiral lamina canal ($p < 0.05$) of the LNC-treated group was significantly weaker than that of the untreated group (Fig. 6A). However, there was no significant difference between the untreated group and the LNC-treated group in nerve fibers innervating IHCs and in cochlear nerve in modiolus ($p > 0.05$).

In the untreated cochlea, S-100 protein is intensively expressed in the nuclei of the spiral limbus, spiral ganglion Schwann cells

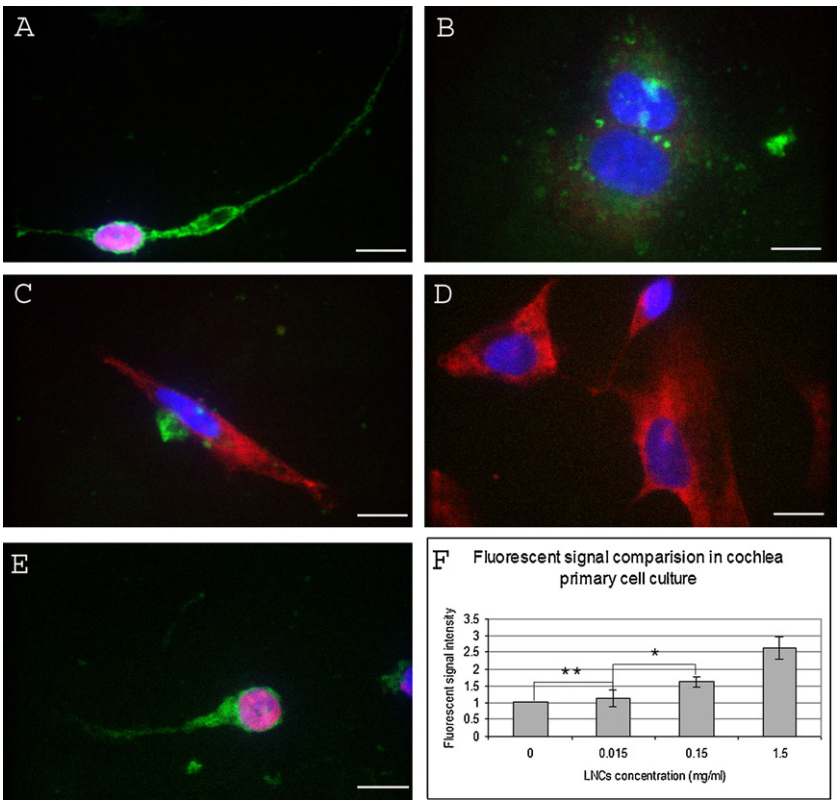

Fig. 2. Concentration-dependant internalization of LNCs in primary rat cochlear cells. Panel A shows intense internalization of LNCs in the cytoplasm induced cell death, which allowed propidium iodide to permeate the nucleus when the cells were exposed to LNCs at a concentration of 1.5 mg/mL. Panel B shows healthy cells with moderate distribution of LNCs in the cytoplasm. These cells rejected propidium iodide when the cells were incubated with LNCs at a concentration of 0.15 mg/mL. Panel C showed sparse internalization of LNCs in the cytoplasm of fibrocytes, with cytosol permeation of propidium iodide when LNCs were added to the medium at a concentration of 0.015 mg/mL. Panel D shows propidium iodide permeation of the cytosol in untreated cells. The neuron in Panel E displays condensed LNCs in the cytoplasm and nuclear permeation of propidium iodide when exposed to LNCs at a concentration of 0.15 mg/mL. Concentration-dependant internalization of LNCs was demonstrated by quantification of the fluorescent signal in the cytoplasm of primary cochlear cells (panel F). (Green: LNCs; red: propidium iodide staining; blue: contrast nuclear staining by DAPI; $^{**}p < 0.01$, $^{*}p < 0.05$, ANOVA). Scale bar = 10 μm.

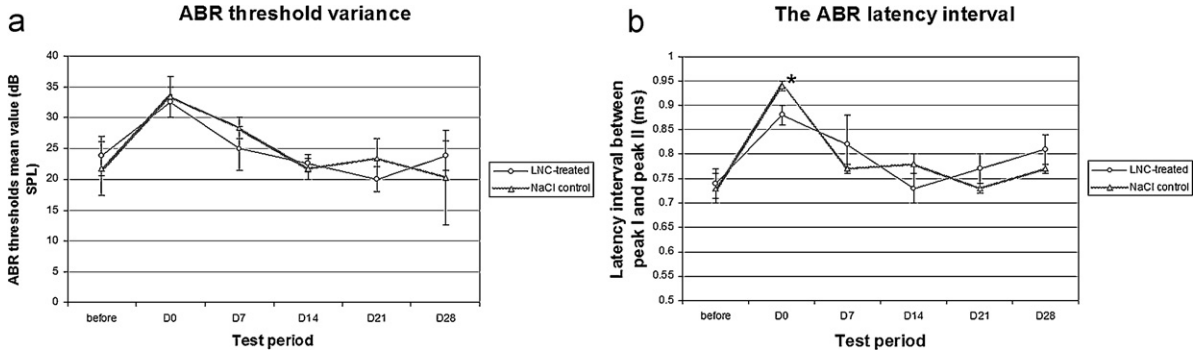

Fig. 3. Dynamic changes in ABR threshold in rats with RWM application of LNCs. The thresholds were elevated immediately after LNC application at D0 in all experimental animals ($^{*}p < 0.05$ of NaCl control). Thresholds returned to baseline at D7 and remained stable up until the final observation time of D28 ($p > 0.05$).

(SGSCs), spiral ligament fibrocytes, and cochlear nerve. Homogeneous distribution of S-100 was also demonstrated in the cytoplasm and nuclei of stria vascularis, inner pillar cells, outer pillar cells, and Deiters' cells of the cochlea (Fig. 5). At D28, the distribution pattern of S-100 in the cochleae of LNC-treated rats was unchanged as compared to that observed in the untreated cochleae. Signal intensities in the LNC-treated group were slightly lower than that of the untreated group without statistic significance ($p > 0.05$, Student's *t*-test) (Fig. 6B).

A typical distribution of synaptophysin was demonstrated within varicosities of efferent endings on the basal pole of the three OHC rows and small dot-like afferent endings at the bottoms of IHCs. The pattern of synaptophysin staining was completely preserved in both the LNC-treated group and the non-treated group. Ribbon synapses were found at the bottoms of IHCs in the LNC-treated and untreated rats [11.83 ± 0.62 (mean ± SEM) and 13.31 ± 1.77 (mean ± SEM) in untreated rats and LNC-treated rats, respectively]. However, this difference was not significant ($p > 0.05$, Student's *t*-test; Fig. 7).

4. Discussion

Concentration-dependent toxicity occurred in the primary cochlear cell culture, with a survival rate of 37.94% among cells

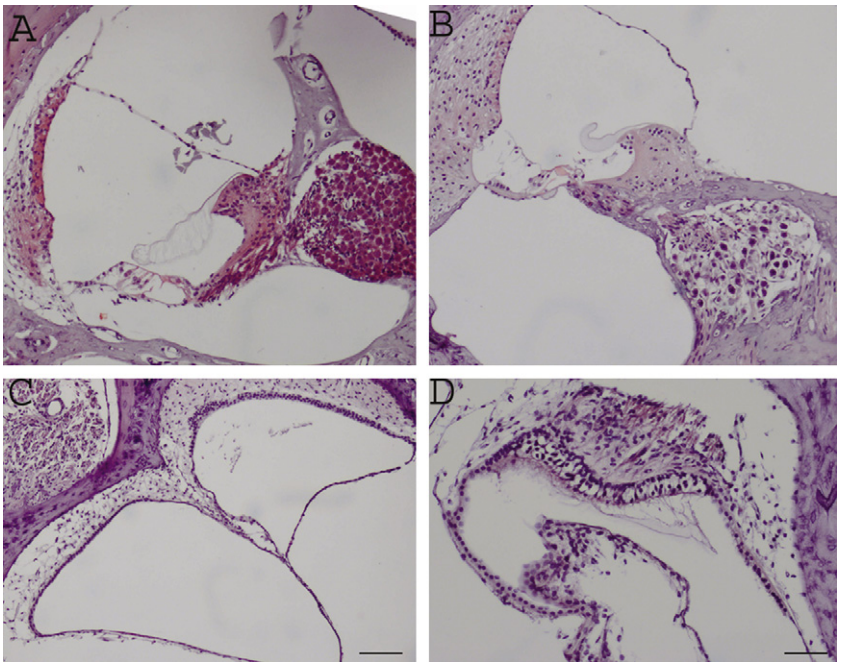

Fig. 4. HE staining of LNC-treated and untreated specimens. The morphology of the inner ear was preserved after LNC treatment. Panels A and B show that IHCs, OHCs and SGCs were preserved in the untreated group (A) and the LNC-treated sample (B). Panels C and D show that the vestibular structure was normal in the untreated group (C), the LNC-treated sample (D).

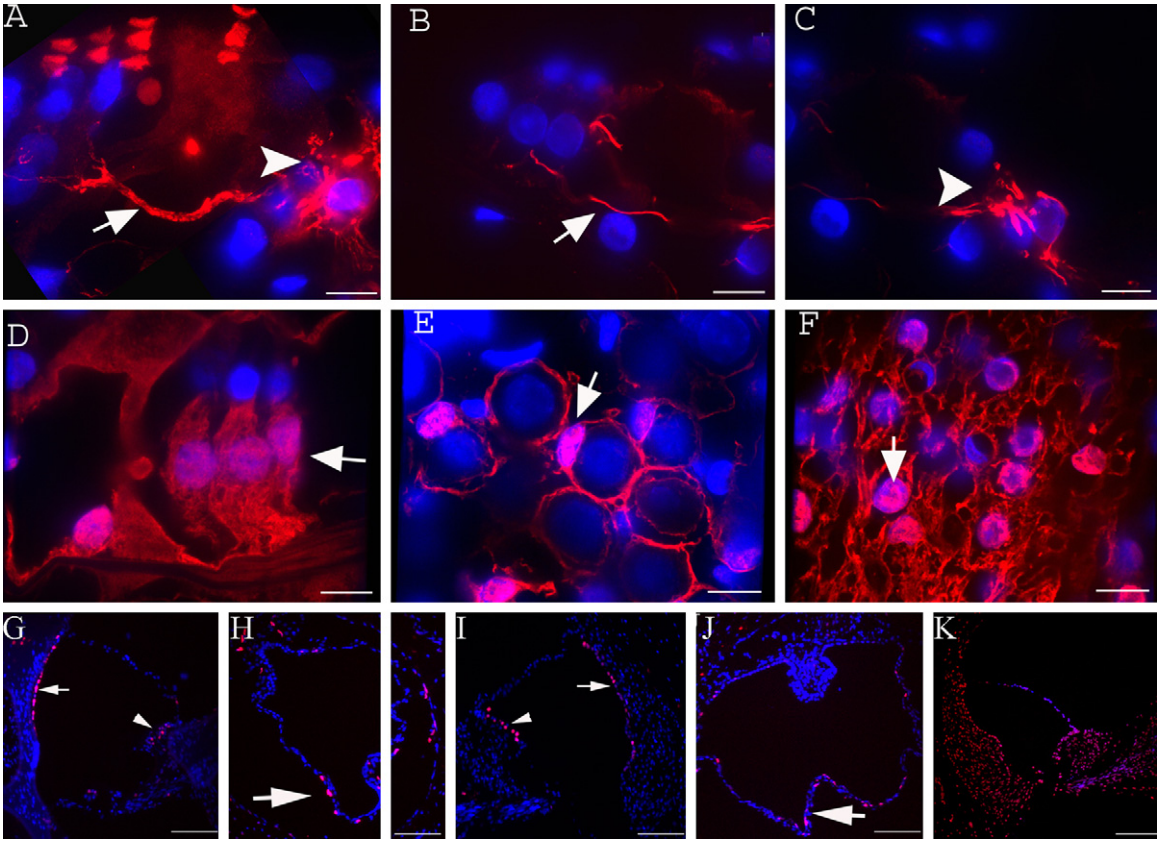

Fig. 5. Immunostaining of neurofilament (NF-200) and S-100 in the rat cochlea at D28 post-RWM application of LNCs. Panel A shows that NF-200-positive nerve fibers innervated IHCs and OHCs of an untreated rat (image made by two confocal stacks of the same specimen). Panels B and C show that NF-200-positive nerve fibers innervated OHCs (B) and IHCs (C) in an LNC-treated rat. Panel D–F demonstrates S-100 staining in Deiters' cells (arrow), Pillar cells (D), SGSCs (E), and spiral ligament fibrocytes (F) of a rat treated with LNCs. Panels G–J demonstrated apoptotic cells showing positive TUNEL staining (red) in the strial marginal cells (arrows in G and I), interdental cells (arrowheads in G and I), and epithelial cells of the semicircular canal (arrows in H and J) (G and H from untreated samples; I and J from LNC-treated samples). Panel K shows universal TUNEL-positivecells in a slice treated by 0.2 μg/mL proteinase K (positive control) (blue: contrast nuclear staining with DAPI). Scale bar = 10 μm.

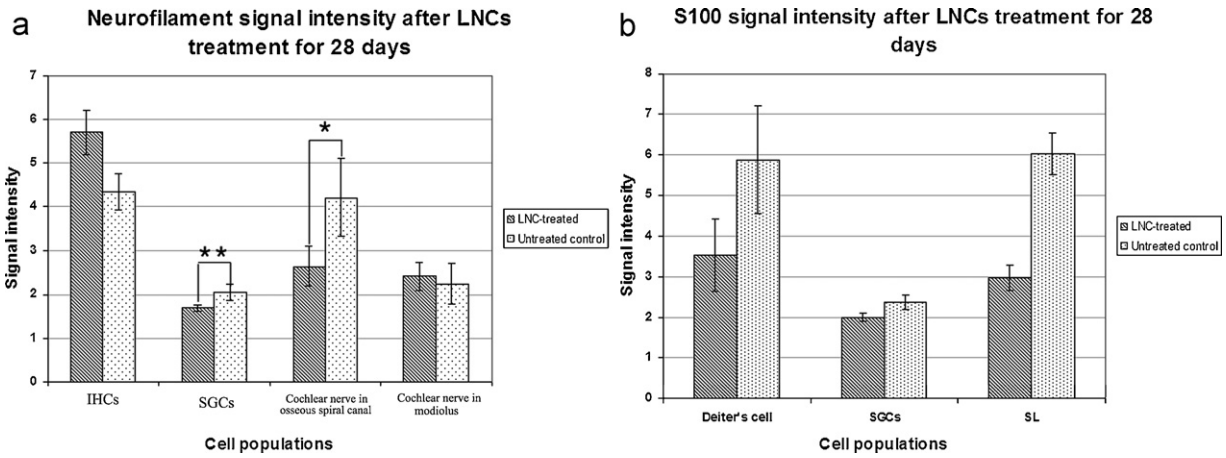

Fig. 6. Quantitative comparison of NF-200 and S-100 expression in LNC-treated and untreated groups. Panel A shows that the NF-200 fluorescent signal in SGCs and in cochlear nerve in osseous spiral lamina canal of LNC-treated rats was significantly weaker than that in un-treated controls (**$p < 0.01$, *$p < 0.05$ Student's t-test). Panel B shows that the S-100 fluorescent signals in Deiter's cells, SGCs and spiral ligament fibrocytes of LNC-treated rats were weaker than that in un-treated controls, but there was not statistic difference ($p > 0.05$, Student's t-test).

treated with 1.5 mg/mL LNCs, whereas the LC_{50} for LNC-treated L929 cells was 2.2 mg/mL. This indicated that certain cell types in primary cochlear cells might be more vulnerable to LNC treatment. Indicating apoptosis or necrosis, the propidium iodide-positive cells in cochlear primary cell culture showed disrupted morphology, it was difficult to distinguish the cell types that were fragile. In the cochlea primary cell culture, the propidium iodide-positive cells always have condensed LNCs in the cytoplasm no matter what concentration of the LNCs in the culture medium. When the NPs occupy certain volume of the cell, the cell function will be impaired, that is called 'nanoparticle overload phenomenon' (Moss, 2006). Toxic effects of the LNCs to L929 cells and cochlea primary cell culture might be due to 'nanoparticle overload phenomenon'.

TUNEL-positive staining observed in interdental cells, stria marginal cells, OHCs, IHCs, and SSC endothelial cells in the untreated inner ear might be caused by either artifact or highly metabolic status. It was reported that TUNEL-positive staining might suggest apoptosis, late necrosis, and autolysis (Gold et al., 1994). Nishizaki and colleagues proved that TUNEL-positive staining in untreated rat inner ear in strial marginal cells, and interdental cells, as well as the epithelial cells of SSCs, IHCs and OHCs, were due to autolysis that occurred during fixation (Nishizaki et al., 1999).

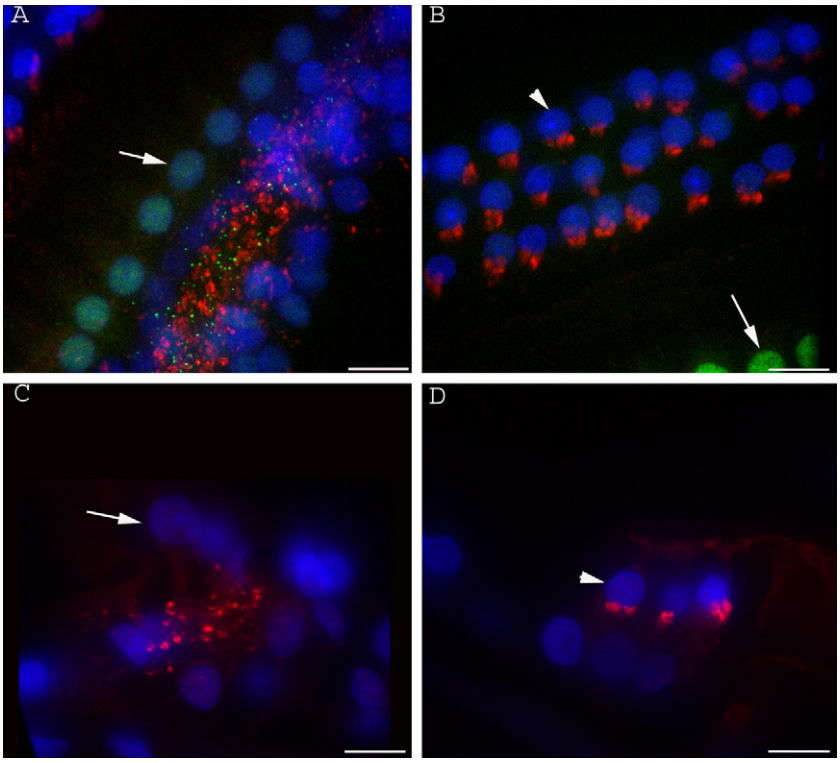

Fig. 7. Immunostaining of synaptophysin and ribbon synapses in rat cochleae treated with LNCs. Panels A and B showed positive staining of synaptophysin and ribbon synapses in Corti's organ at 2 h post-RWM administration of LNCs (confocal stacks). Panels C and D showed positive staining of synaptophysin below IHCs and OHCs at D28 post-RWM application of LNCs. (Arrow: IHC nucleus; arrowhead: OHC nucleus; green: ribbon synapses; red: synaptophysin; blue: contrast nuclear staining with DAPI) Scale bar = 10 μm.

Our previous study on guinea pig inner ear treated with mitochondrial toxin showed TUNEL-positive staining not only in strial marginal cells and epithelial cells of SSCs which were detected in untreated inner ear too, but also in spiral ligament fibrocytes, Reissner's membrane, mesothelial cell of scala tympani and OHCs which induced by toxic effect of mitochondrial toxin (Zou et al., in press). Therefore we interpreted that the TUNEL-positive staining of the cells in our present results was not caused by LNC treatment in the rat inner ear.

ABR threshold shift occurred at D0 in both LNC treatment and no treatment groups, which recovered at D7 and remained stable throughout the 4-week observation period in every group. This transient changes in ABR threshold might be caused by the surgical disturbance to the conducting system in the middle ear but not cochlear impairment, which was further verified by quantifying the IHC of ribbon synapses of IHC and the distribution pattern of synaptophysin in both IHC and OHC of rat cochlea at D0 (2 h after LNC administration). IHC encode stimuli with graded changes in membrane potential and transmit the signal through ribbon synapses to drive action potentials in associated afferent neurons. Ribbon synapses contribute to a particular feature of release: the latency and precision of spike timing in the postsynaptic afferent neurons (Nouvian et al., 2006; Zenisek et al., 2004). CtBP2 (C-terminal binding protein 2), a synaptic ribbon marker, is supposed to mark the sites of vesicle fusion and transmitter release in afferent nerve terminals. Ribbon synapses are composed of vesicles tethered by fine filaments to each face of a synaptic ribbon, whether in the IHCs and vestibular hair cells or in photoreceptors and bipolar cells in the retina (Nouvian et al., 2006; Zenisek et al., 2004). The intensity of ribbon synapse is related to the sensitivity of the mammalian cochlea (Meyer et al., 2009). In the present study, the quantity of ribbon synapses was not affected by LNC treatment. Synaptophysin is an important synaptic protein for hair cell physiology and often disintegrates before hair cell death (Maria Visitación Bartolome et al., 2009). Synaptophysin is located in medial efferent nerve endings, which innervate OHCs, and in lateral efferent nerve endings, which innervate IHCs. In this study, synaptophysin within varicosities of efferent endings was observed under the OHCs (Fig. 7B and D), and a dot-like pattern of synaptophysin staining was observed in nerves innervating the IHCs (Fig. 7A and C). The pattern of synaptophysin staining was completely preserved in OHCs and IHCs of LNC-treated cochleae.

Neurofilament 200 (NF-200) is a structural protein that supports the architecture of peripheral and central axons (Hoffman and Lasek, 1975) and plays a role in axonal transport (Miller et al., 2002). It is a reliable marker for myelinated afferent neurons. NF-200 immunostaining is used frequently in diagnosing neurodegenerative diseases (Talja et al., 2009); many neurodegenerative diseases are marked by the absence or degradation of NF-200 (Hwang et al., 2005; Posmantur et al., 1994; Posmantur et al., 2000). Positive NF-200 staining was found in the periphery of SGCs projecting to IHCs and OHCs (Fig. 5B and C). In SGCs and cochlear nerve in osseous spiral lamina canal, NF-200 levels were lower than the untreated control (Fig. 6A), whereas, hearing of the rats was not affected at D28. These changes need to be verified in future investigations.

S-100 is a marker of spiral ganglion Schwann cells. Hurley and colleagues observed S-100 immunolabeling in inner sulcus cells, inner phalangeal cells, spiral ligament, spiral limbus, and intermediate cells (Hurley et al., 2007). In addition to these locations, we also detected S-100 immunolabeling in Deiters' cells, spiral ganglion Schwann cells (SGSCs), and the cochlear nerve. S-100 is extensively expressed in the nucleus and moderately expressed in cytoplasm. The S-100 distribution was not affected by LNC treatment, but the immunostaining intensities in Deiter's cells, SGSCs and spiral ligament fibrocytes of the LNC-treated rats were lower than that of the untreated group. The mechanism is unknown. It was reported that S-100 proteins are secreted from cells on stimulation, exerting cytokine- and chemokine-like activities. Pathologic level leads to sustained activation, cell death and disease (Claus W Heizmann, 2005). However, the decreased secretion of S-100 proteins observed in the present study can rule out the potential pathological response. These changes might be caused by the age related modification on the Ca^{2+}-homeostasis regulation system in the cochlea, which needs to be investigated in the future.

5. Conclusion

In conclusion, cncentration-dependent toxicity occurred in the primary cochlear cell culture and mouse fibroblasts. When applied to the middle ear cavity, LNCs did not cause hearing impairment, cell death, or morphological changes in the inner ear. Cochlear neural elements, such as synaptophysin, ribbon synapses, and neurofilament-200, were not affected by the administration of LNCs. However, the expression of S-100 decreased in spiral ligament fibrocytes and spiral ganglion cells after LNC delivery, a result that requires further investigation. LNCs are therefore potential vectors for drug delivery to the inner ear.

Acknowledgments

This study was supported by the European Community 6th Framework Programme on Research, Technological Development and Demonstration (Nanotechnology-based Targeted Drug Delivery. Contract number: NMP4-CT-2006-026556, Project acronym: NANOEAR).

References

Bedrosian, J.C., Gratton, M.A., Brigande, J.V., Tang, W., Landau, J., Bennett, J., 2006. In vivo delivery of recombinant viruses to the fetal murine cochlea: transduction characteristics and long-term effects on auditory function. Mol. Ther. 14, 328–335.

El-Hakim, H., Abdolell, M., Mount, R.J., Papsin, B.C., Harrison, R.V., 2002. Influence of age at implantation and of residual hearing on speech outcome measures after cochlear implantation: binary partitioning analysis. Ann. Otol. Rhinol. Laryngol. 189, 102–108.

Florea, B.I., Meaney, C., Junginger, H.E., Borchard, G., 2002. Transfection efficiency and toxicity of polyethylenimine in differentiated Calu-3 and nondifferentiated COS-1 cell cultures. AAPS PharmSci. 4, E12.

Gantz, B.J., Woodworth, G.G., Knutson, J.F., Abbas, P.J., Tyler, R.S., 1993. Multivariate predictors of audiological success with multichannel cochlear implants. Ann. Otol. Rhinol. Laryngol. 102, 909–916.

Geers, A., Brenner, C., Nicholas, J., Uchanski, R., Tye-Murray, N., Tobey, E., 2002. Rehabilitation factors contributing to implant benefit in children. Ann. Otol. Rhinol. Laryngol. 189, 127–130.

Gold, R., Schmied, M., Giegerich, G., Breitschopf, H., Hartung, H.P., Toyka, K.V., Lassmann, H., 1994. Differentiation between cellular apoptosis and necrosis by the combined use of in situ tailing and nick translation techniques. Lab. Invest. 71, 219–225.

Heizmann, C.W., 2005. The importance of calcium-binding proteins in childhood diseases. J. Pediatr. 147, 731–738.

Hoffman, P.N., Lasek, R.J., 1975. The slow component of axonal transport. Identification of major structural polypeptides of the axon and their generality among mammalian neurons. J. Cell Biol. 66, 351–366.

Horie, R.T., Sakamoto, T., Nakagawa, T., Tabata, Y., Okamura, N., Tomiyama, N., Tachibana, M., Ito, J., 2010. Sustained delivery of lidocaine into the cochlea using poly lactic/glycolic acid microparticles. Laryngoscope 120, 377–383.

Hureaux, J., Lagarce, F., Gagnadoux, F., Clavreul, A., Benoit, J.P., Urban, T., 2009. The adaptation of lipid Nan capsule formulations for blood administration in animals. Int. J. Phytoremediation 379, 266–269.

Hureaux, J., Lagarce, F., Gagnadoux, F., Rousselet, M.C., Moal, V., Urban, T., Benoit, J.P., 2010. Toxicological study and efficacy of blank and paclitaxel-loaded lipid nanocapsules after i.v. administration in mice. Pharm. Res. 27, 421–430.

Hurley, P.A., Crook, J.M., Shepherd, R.K., 2007. Schwann cells revert to non-myelinating phenotypes in the deafened rat cochlea. Eur. J. Neurosci. 26, 1813–1821.

Huynh, N.T., Passirani, C., Saulnier, P., Benoit, J.P., 2009. Lipid nanocapsules: a new platform for nanomedicine. Int. J. Phytoremediation 379, 201–209.

Hwang, I.K., Koh, U.S., Lee, J.C., Yoo, K.Y., Song, J.H., Jung, J.Y., Nam, Y.S., Lee, I.S., Kang, T.C., Won, M.H., 2005. Transient ischemia-induced changes of neurofilament 200 kDa immunoreactivity and protein content in the main olfactory bulb in gerbils. J. Neurol. Sci. 239, 59–66.

Jager, E., Venturini, C.G., Poletto, F.S., Colome, L.M., Pohlmann, J.P., Bernardi, A., Battastini, A.M., Guterres, S.S., Pohlmann, A.R., 2009. Sustained release from lipid-core nanocapsules by varying the core viscosity and the particle surface area. J. Biomed. Nanotechnol. 5, 130–140.

Luebke, A.E., Foster, P.K., Muller, C.D., Peel, A.L., 2001. Cochlear function and transgene expression in the guinea pig cochlea, using adenovirus- and adeno-associated virus-directed gene transfer. Hum. Gene Ther. 12, 773–781.

Maria Visitación Bartolome, Francisco Carricondo, P.Z., Gil-Loyzaga, Pablo, 2009. Immunocytochemical detection of synaptophysin in C57BL/6 mice cochlea during aging process. Brain Res. Rev. 60, 341–348.

Meyer, A.C., Frank, T., Khimich, D., Hoch, G., Riedel, D., Chapochnikov, N.M., Yarin, Y.M., Harke, B., Hell, S.W., Egner, A., Moser, T., 2009. Tuning of synapse number, structure and function in the cochlea. Nat. Neurosci. 12, 444–453.

Miller, C.C., Ackerley, S., Brownlees, J., Grierson, A.J., Jacobsen, N.J., Thornhill, P., 2002. Axonal transport of neurofilaments in normal and disease states. Cell. Mol. Life Sci. 59, 323–330.

Moss, O., 2006. Insights into the health effects of nanoparticles: why numbers matter. CIIT Activities 26, 1–8.

Nishizaki, K., Yoshino, T., Orita, Y., Nomiya, S., Masuda, Y., 1999. TUNEL staining of inner ear structures may reflect autolysis, not apoptosis. Hear. Res. 130, 131–136.

Nouvian, R., Beutner, D., Parsons, T.D., Moser, T., 2006. Structure and function of the hair cell ribbon synapse. J. Membr. Biol. 209, 153–165.

Osberger, M.J., Zimmerman-Phillips, S., Koch, D.B., 2002. Cochlear implant candidacy and performance trends in children. Ann. Otol. Rhinol. Laryngol. 189, 62–65.

Posmantur, R., Hayes, R.L., Dixon, C.E., Taft, W.C., 1994. Neurofilament 68 and neurofilament 200 protein levels decrease after traumatic brain injury. J. Neurotrauma 11, 533–545.

Posmantur, R.M., Newcomb, J.K., Kampfl, A., Hayes, R.L., 2000. Light and confocal microscopic studies of evolutionary changes in neurofilament proteins following cortical impact injury in the rat. Exp. Neurol. 161, 15–26.

Pyykko I., Dalton P., 2009. NANOEAR: 3g-nanotechnology based targeted drug delivery using the inner ear as a model target organ, http://www.nanoear.org/ (online).

Scheper, V., Wolf, M., Scholl, M., Kadlecova, Z., Perrier, T., Klok, H.A., Saulnier, P., Lenarz, T., Stover, T., 2009. Potential novel drug carriers for inner ear treatment: hyperbranched polylysine and lipid nanocapsules. Nanomedicine (London, England) 4, 623–635.

Smolewski, P., Grabarek, J., Halicka, H.D., Darzynkiewicz, Z., 2002. Assay of caspase activation in situ combined with probing plasma membrane integrity to detect three distinct stages of apoptosis. J. Immunol. Methods 265, 111–121.

Talja, I., Reimand, T., Uibo, O., Reimand, K., Aun, S., Talvik, T., Janmey, P.A., Uibo, R., 2009. Antibodies to neurofilaments. Ann. N. Y. Acad. Sci. 1173, 130–136.

Tan, B.T., Foong, K.H., Lee, M.M., Ruan, R., 2008. Polyethylenimine-mediated cochlear gene transfer in guinea pigs. Arch. Otolaryngol. Head Neck Surg. 134, 884–891.

Zenisek, D., Horst, N.K., Merrifield, C., Sterling, P., Matthews, G., 2004. Visualizing synaptic ribbons in the living cell. J. Neurosci. 24, 9752–9759.

Zou, J., Saulnier, P., Perrier, T., Zhang, Y., Manninen, T., Toppila, E., Pyykko, I., 2008. Distribution of lipid nanocapsules in different cochlear cell populations after round window membrane permeation. J. Biomed. Mater. Res. 87, 10–18.

Zou, J., Li, M., Zhang Y., Zheng, G., Chen D., Chen S., Zheng, H., in press. Transport augmentation through the blood-inner ear barriers of guinea pigs treated with 3-nitropropionic acid and patients with acute hearing loss, visualized with 3.0 T MRI. Otol. Neurotol.